Cellular Noise and The Aging Process

Tommy Begay[†], Nick Dowdall[‡], Mat Gluck[§], Olaoluwa Okunola[¶]

Abstract

It is generally accepted among scientists that cellular aging is an irreversible process that is poorly understood. Several theories, including telomere shortening, mitotic misregulation, free radical theory and many others, have been proposed as possible explanations for this phenomenon. Recently, Bennett-Baker *et al*[3], observed a correlation between the reactivation of genes on inactive X-chromosomes and age in female mice. Motivated by these studies, we propose two mathematical models to investigate the progression of aging at the cellular level. In the first approach, we study the dynamics of aging using a discrete time dynamical system based on competition between "noisy" and "noise-free" cells. Our preliminary results suggest the existence of three different qualitative outcomes. These outcomes are best described by exclusion and coexistence, where coexistence occurs under two dynamically distinct scenarios. In order to incorporate a more biologically accurate framework, we also consider a stage-structured model that incorporates stage dependent vital rates. These are important as the rates change with the accumulation of "noise".

1 Introduction

Aging has been a topic of great interest to scientists for many years. The definition of aging is rarely agreed upon by researchers but includes all time-dependent processes that occur within an organism whether adverse or not. Often, in biological literature, aging is more narrowly referred to as the gradual and irreversible decrease in function of a system of cells with time [1]. Over the years, many theories on aging have been developed and tested in an effort to better understand this process. These theories include the telomere shortening theory [12], the predetermined life span theory [2], the cross linking theory [14], and the free radical theory [13]. Two closely related theories of aging are the predetermined life span theory and the telomere shortening theory. The predetermined life span theory claims that an organism has a given amount of time to live which is predetermined in the embryonic cell. Furthermore, this theory says that the amount of time for an organism to live is based on the number of cell divisions the organism's cells undergo [2]. The telomere shortening theory suggests that the shortening of

[†]Arizona State University
[‡]Santa Rosa Junior College
[§]University of California at Riverside
[¶]University of the District of Columbia

telomeres, which occurs at each cell division (mitosis), may be responsible for aging. This gradual change in length of the telomeric DNA causes changes in the proteins around the telomere, which can lead to a change in the gene expression of the entire chromosome [10]. Altered gene expression will cause altered and potentially non-functional cells, which will, in turn, lead to aging. As a result, some scientists now view telomeres as cellular timers that trigger cells to cease function when time runs out [11].

Other related aging theories are the cross linking and the free radical theories. The free radical theory [13] was developed in 1956 and suggests that highly unstable molecules, called free radicals (denoted by *f.r.'s*) are produced as a by product of metabolic processes [3]. These free radicals can sometimes escape their neutralization processes and cause cellular damage [5]. Since the mitochondria are the primary sites for free radical production, mitochondrial DNA (*mtDNA*), which is not readily repaired, is most subject to *f.r.* damage. As a result, *mtDNA* damage accumulates and cell energy production declines, thus causing cell death and aging [6]. The cross linking theory claims that aging is due to two or more large molecules becoming bound together. These large, nonfunctional molecules, in theory, will accumulate in the cell and cause cellular and tissue damage in numerous ways including decreasing tissue elasticity and impeding intra- and inter-cellular transport [8]. Also, some cross-linked molecules have been shown to reduce the degradation of proteins (which is necessary to eliminate nonfunctional proteins) [7] and increase the number of free radicals produced by 50 times the normal rate [12]. Thus, one can infer that the free radical theory of aging picks up where the cross linking theory leaves off.

The common themes in the above mentioned theories are DNA and gene expression. Recent studies by Ly *et al.,* [12] and Bennett-Baker *et al.,* [3] suggest a possible explanation for all of the previously mentioned theories. Both studies show that as age increases, gene expression patterns change. These changes could be the source of the theories discussed above. Ly *et al* [12] suggest that as age increases, the genes whose products regulate the cell cycle and aging tend to become expressed in a way that promotes aging [13]. Bennett-Baker *et al* [3] show that as age increases, certain genes that were initially inactivated start to become expressed [3].

The motivation of this study is to answer the following question: How do these gene expression patterns change with time? In particular, we propose to add to the body of work that may eventually corroborate the work of Bennett-Baker *et al* [3] using both a discrete time competition model and a stage structured model. Through analytical and numerical analyses of these models we hope to suggest gene expression patterns for cohorts for which no data was collected, while fitting the existing data of the work carried out by Bennett-Baker *et al* [3] (See illustration A). Furthermore, we show the possibility of coexistence of cells of different types, under conditions that would be impossible in classical competition systems.

This study is structured as follows. Section 2 explains the methods used in the work of Bennett-Baker and her team [3]. Section 3 introduces the general Leslie-Gower competition model and Section 4 applies the general Leslie-Gower model to a population of cells characterized by error and error-free classes; Section 5 carries out the analysis of this specific case model while Section 6 explores the sensitivity of the parameter values that are found to be necessary for the existence of multiple equilibria and the corresponding stability discussed in the analysis.

Finally, Section 7 summarizes our results and provides a discussion of current and future work.

2 Experimental Methods

In their report, "Age-associated activation of epigenetically repressed genes in the mouse," Bennett-Baker *et al.*[3] quantitatively describe changes in epigenetic regulation in animals. To do this, they track the gene *Atp7a*, a gene that is subject to X chromosome inactivation in female mice. X chromosome inactivation is a well-studied mammalian epigenetic system. Quantitative measurements of RNA transcripts from different alleles were made in mice whose ages ranged form two to twenty four months. The quantity measured in this study was X_i/X_a, the ratio of genes expressed from the inactive chromosome to genes expressed from the active chromosome. The results showed that for some cohorts, the mean increase of this ratio was up to 2.2%. A more detailed description of the experimental methods can be found in [3].

3 General Leslie-Gower Model

Interaction between similar species can lead to competition for a limited resource. Depending on the strength between species interaction (interspecific competition), competitive exclusion is a possible stable asymptotic dynamic outcome (deterministically). However, if the competition between species is sufficiently weak, then the long term competitive outcome may be best described by species coexistence. These notions stem from classical competition theory, which are based on the Lotka-Volterra differential equations. Similar competitive predictions have been determined for discrete systems. One such system, the Leslie-Gower model, was used to understand the dynamics of competing species of flour beetles (*Tribolium*). This model is a 2D system of difference equations (a modification of the Beverton-Holt equation) given by:

$$\begin{aligned} x_{t+1} &= \frac{x_t b_x}{1 + c_{11}x_t + c_{12}y_t}, \\ y_{t+1} &= \frac{y_t b_y}{1 + c_{21}x_t + c_{22}y_t}. \end{aligned} \tag{1}$$

The parameter values b_x and b_y denote the average number of births per generation for species x and y respectively. The parameter c_{ij} represents the competition coefficient (effect) of species j on species i for $i, j = 1, 2$. For example, c_{11} describes the competition species x exerts on itself. Competition with $i = j$ is termed intraspecific competition, while that with $i \neq j$ is interspecific competition. The global dynamics have been fully studied for the Leslie-Gower model and the results can be found in [5]. Interestingly, similar to Lotka-Volterra competitive outcomes, a necessary condition for species coexistence is $c_{11}c_{22} > c_{12}c_{21}$ as depicted in Illustration 1.

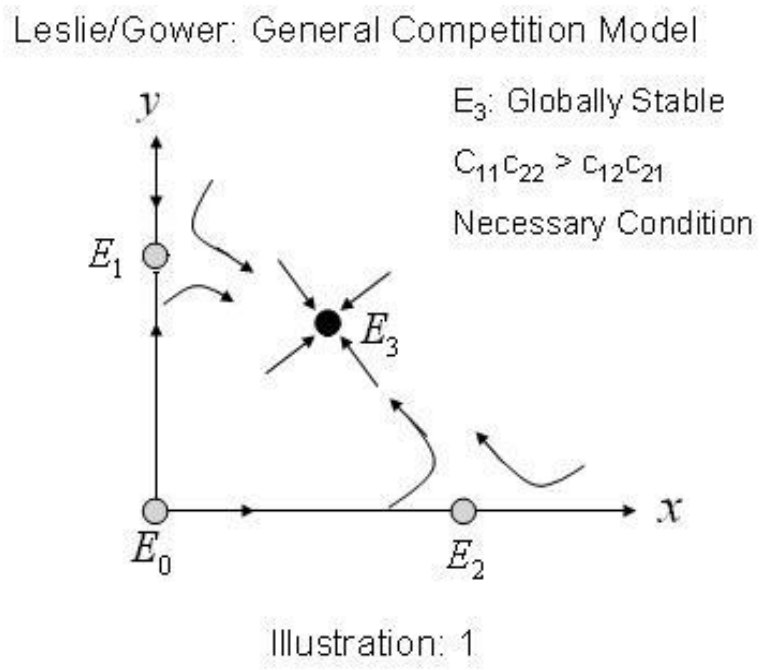

Figure 1: One stable positive equilibrium (E_3) exists and is globally stable while, E_0, E_1, E_2 are all unstable.

4 Discrete Cell-Aging Model

In this section the framework of the Leslie-Gower model is modified to study the competitive dynamics of a system in which the populations are the results of either error-free (P) reproduction or not(Q). The modified model is:

$$\begin{aligned} P_{t+1} &= \frac{amP_t}{1 + c_{11}P_t + c_{12}Q_t}, \\ Q_{t+1} &= \frac{a(1-m)P_t + bQ_t}{1 + c_{21}P_t + c_{22}Q_t}. \end{aligned} \tag{2}$$

In this model it is assumed that $a = \alpha(1-\mu_a)$ is the product of the average number of births per generation for cells born into class P_t and the probability of survival for class P_t ($0 < a \leq 2$). $b = \beta(1-\mu_b)$ is the product of the average number of births per generation for cells born into class Q_t and probability of survival for class Q_t ($0 < b \leq 2$). The parameters c_{ij} describe the competition factors in the general case ($0 < c_{ij} < 1$) and m is the probability that a cell in class P_t will produce a cell in class P_t ($0 < m < 1$).

The introduction of m gives rise to a new type of interaction that was not being considered in the Leslie-Gower model. Note that in the equation for Q_{t+1} there is a probability that a cell in class P_t will produce a cell in class Q_t. This would be equivalent to a competition model

between two species A and B, where species A has the capability of giving birth to a member of species B. While this may not generally make biological sense, this is a unique feature of cellular biology where error-free cells can produce cells that possess error.

5 Equilibria and Stability of the Cell-Aging Model

To gather insight as to the dynamics of (2), standard dynamical systems techniques will be employed. This type of qualitative analysis entails finding equilibria (fixed points) and establishing their associated stability properties. Stability of the equilibria can be determined by the magnitude of eigenvalues of the Jacobian matrix of the map evaluated at these fixed points (each of which will be denoted by E_i).
The Jacobian of system (2) is given by:

$$J = \begin{pmatrix} \dfrac{am(1+c_{12}Q)}{(1+c_{11}P+c_{12}Q)^2} & \dfrac{-amc_{12}P}{(1+c_{11}P+c_{12}Q)^2} \\ \dfrac{a(1-m)(1+c_{22}Q)-bc_{21}Q}{(1+c_{21}P+c_{22}Q)^2} & \dfrac{b(1+c_{21})P-ac_{22}(1-m)P}{(1+c_{21}P+c_{22}Q)^2} \end{pmatrix} \tag{3}$$

For local asymptotic stability of E_i, all eigenvalues of the Jacobian at E_i (J^*) must lie inside the unit disk (i.e. $|\lambda_{1,2}| < 1$). Equivalently, necessary and sufficient conditions for $|\lambda_{1,2}| < 1$ are the Jury conditions ($|trJ^*| < 1 + detJ^* < 2$) [4]. To find the fixed points of (2), we seek ordered pairs of the form $(\bar{P}, \bar{Q})$ such that $P_{t+1} = P_t = \bar{P}$ and $Q_{t+1} = Q_t = \bar{Q}$. By inspection of (2), one such equilibrium point is given by the trivial solution $E_0 = (0, 0)$. Similarly, substituting $\bar{P} = 0$ and with $\bar{Q} > 0$ yields, $\bar{Q} = \dfrac{b-1}{c_{22}}$ (i.e. $E_1 = (0, \dfrac{b-1}{c_{22}})$). Positive equilibria, $\bar{P} > 0$ and $\bar{Q} > 0$, are also possible and their existence will be discussed later.
Stability of $E_0 = (0, 0)$
Substituting E_0 into (3) yields a triangular matrix with eigenvalues $\lambda_1 = am$ and $\lambda_2 = b$. Therefore, E_0 is LAS when $|am| < 1$ and $|b| < 1$. Biologically, the trivial equilibrium corresponds to the extinction of both P and Q and is stable when both of these classes are not reproducing fast enough to replace themselves.

Stability of $E_1 = (0, \dfrac{b-1}{c_{22}})$
This fixed point lies on the Q-axis if $b > 1$ indicating the exclusion of P cells. Substituting E_1 into the Jacobian, it is found that the eigenvalues of the Jacobian are given by $\lambda_1 = \dfrac{am}{1+\frac{c_{12}}{c_{22}}(b-1)}$ and $\lambda_2 = \dfrac{1}{b}$. Therefore, the two conditions guaranteeing LAS of E_1 are $b > 1$,which also guarantees the existence of E_1, and $(am-1) < \frac{c_{12}}{c_{22}}(b-1)$. That is, in order for the Q cells to exclude the P cells, the average number of births per cell into class Q, given by b, must be greater than 1. As a result, when $b > 1$, when E_1 comes into existence, E_0 becomes unstable. The other condition for LAS of E_1,

$$(am-1) < \frac{c_{12}}{c_{22}}(b-1), \tag{4}$$

will prove to be an important inequality which will reappear when determining the existence of positive fixed points. The phase plane incorporating E_0 and E_1 is displayed in Illustration 2.

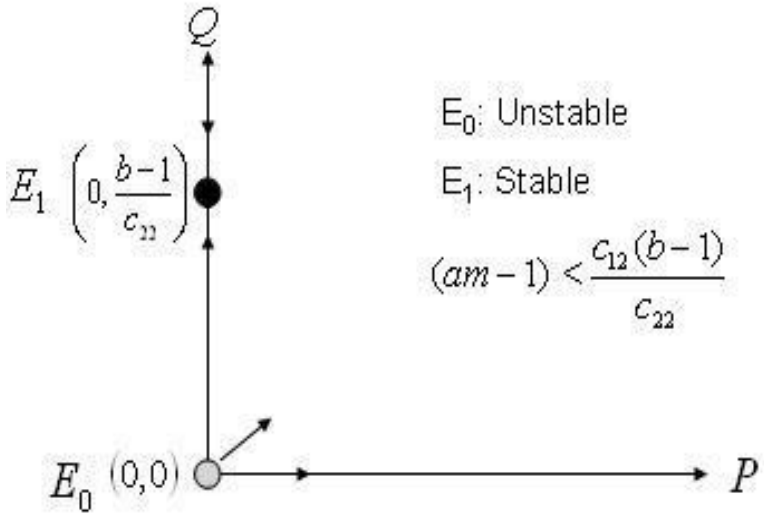

Illustration: 2

Existence of E_2 and E_3

We will now explore conditions for which positive equilibria exist (i.e. ordered pairs $(\bar{P}, \bar{Q})$ which lie in the positive cone). Assuming $\bar{P} > 0$, we have the following expression for $\bar{P}$ in terms of $\bar{Q}$:

$$\bar{P} = \frac{am - 1 - c_{12}\bar{Q}}{c_{11}}. \tag{5}$$

Substituting (5) into the equation for $\bar{Q}$ yields a quadratic in $\bar{Q}$ given by:

$$A\bar{Q}^2 + B\bar{Q} + C = 0. \tag{6}$$

Solutions of (6) are given by:

$$\bar{Q}_{+,-} = \frac{-B \pm \sqrt{B^2 - 4AC}}{2A},$$

where A, B, and C are defined by:

$$A = c_{11}c_{22} - c_{12}c_{21},$$
$$B = -c_{11}(b-1) + c_{12}a(1-m) + c_{21}(am-1),$$
$$C = -a(1-m)(am-1).$$

Biologically, only real, positive equilibria are considered, ($\bar{P}, \bar{Q} \in \mathbb{R}^+$). Inspecting (5), we require $(am-1) > 0$ for the possibility of positive equilibria. Since m represents a "probability", we have $m \in [0,1]$ (or $(1-m) > 0$). These conditions force $C < 0$ for the existence of positive equilibria. Thus, for existence, satisfying $C < 0$ and $B^2 - 4AC > 0$ (to avoid complex conjugate solutions will be considered). A geometric argument is used to outline conditions for the existence of zero, one and two positive fixed points as below.

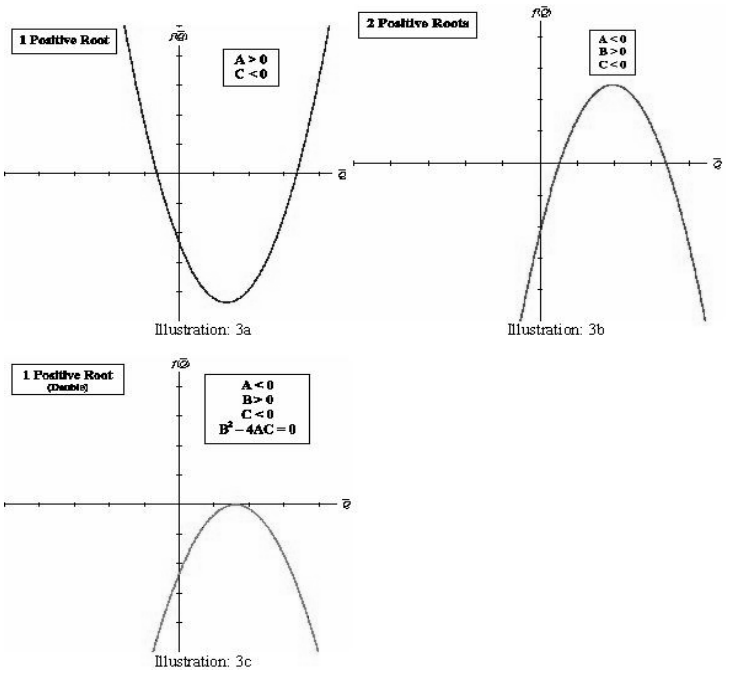

Case 1: Exactly One Positive Fixed Point (E_2) Using the Illustration 3a, it is apparent from the graph that:

$$A > 0$$
$$C < 0.$$

The only positive solution is given by $\bar{Q}_1 = \frac{-B+\sqrt{B^2-4AC}}{2A}$. To obtain a corresponding positive $\bar{P}_1$ we have:

$$\bar{P}_1 = \frac{am - 1 - c_{12}\bar{Q}_1}{c_{11}} > 0 \quad \Longleftrightarrow \quad \bar{Q}_1 < \frac{am-1}{c_{12}}.$$

This algebraically simplifies to

$$(am-1) < \frac{c_{12}}{c_{22}}(b-1).$$

When this condition holds, E_2 exists in the first quadrant. This condition contradicts the stability condition for E_1. If we apply the same biological argument as we did for E_1, we must have $c_{22} < c_{12}$, which says that intra-specific competition must be greater than the inter specific competition to have coexistence. This result agrees with the results of the Leslie-Gower model. When analyzing the stability of E_2, we find that the determinant of the Jacobian evaluated at E_2, is intractable, thus we look for numerical solutions. Upon doing this, we find that all eigenvalues are less than one in modulus for every set of biologically plausible parameters. This leads us to believe that E_2 is locally stable, although we do not attempt to prove this result.

Case 2: Two Positive Fixed Points (E_2) and (E_3) Using Illustration 3b, we see that we

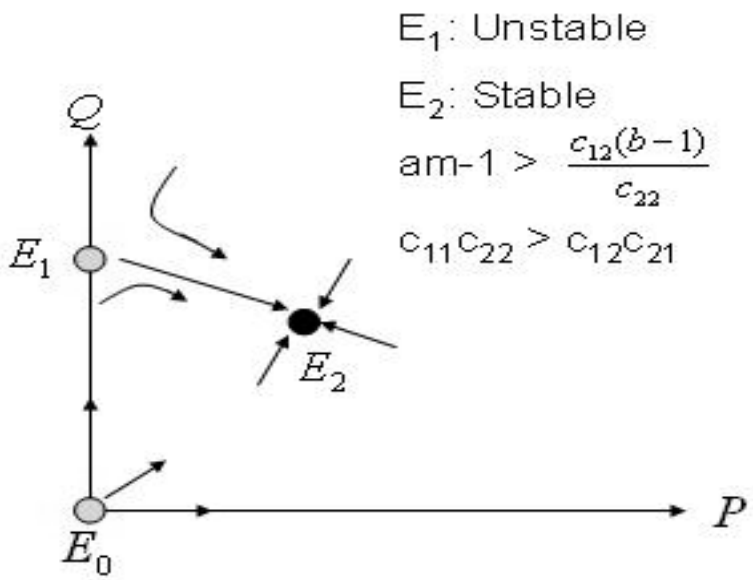

Illustration: 4

must have:

$$\begin{aligned} A &< 0 \\ B &> 0 \\ C &< 0. \end{aligned}$$

Since both $\bar{Q}_1$ and $\bar{Q}_2$ are positive, each is substituted into (5). Doing this, we find that both of the corresponding values of $\bar{P}$ are positive whenever

$$(am-1) < \frac{c_{12}}{c_{22}}(b-1).$$

When this is satisfied E_1 is LAS. Thus, we have that whenever E_2 and E_3 exist simultaneously in the first quadrant, E_1 is locally stable. When examining the stability of E_2 and E_3, a Jacobian with an intractable determinant is obtained. So again, we replace the parameters with biologically appropriate values to make the determinant of the Jacobian manageable. After doing this, we find that for E_2, one eigenvalue is greater than one, while the other is less than one for each set of biologically plausible parameters. This proves that E_2 is a saddle node. Using this same process for E_3, we find that both eigenvalues are both less than one for every case that we tested. From this we suspect that E_3 is locally asymptotically stable. Again, we do not attempt to prove the local dynamics of E_2 or E_3. The local dynamics of this situation are shown in Illustration 4.

Case 3: Coalescence of the Two Fixed Points (E_2) and (E_3)

Examining Illustration 3c, one notices that the fixed points coalesce when there is one positive root as a double root. Conditions for this occurrence are as follows:

$$\begin{aligned} A &< 0 \\ B &> 0 \\ C &< 0 \\ B^2 - 4AC &= 0. \end{aligned}$$

These conditions are identical to the conditions of Case 2, with the additional constraint that the discriminant of the quadratic solution $\bar{Q}$ is zero. This reduces the two fixed point solutions to $\bar{Q} = \frac{-B}{2A}$.

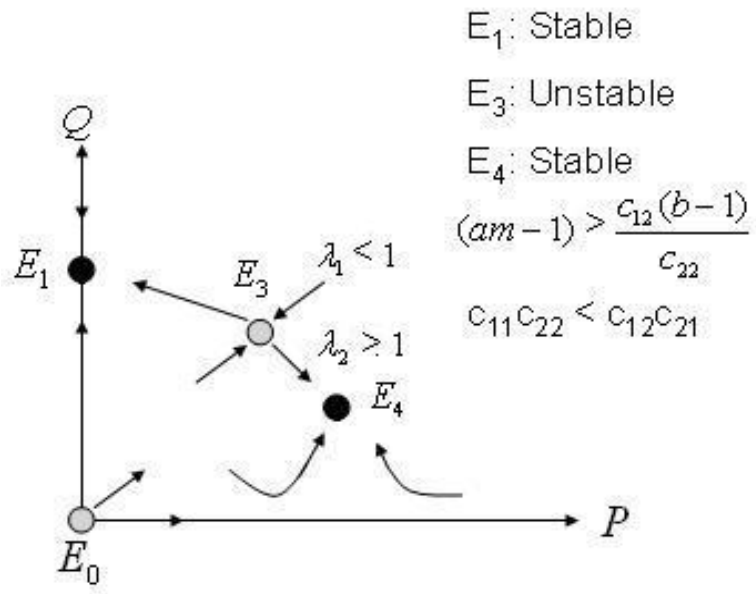

Illustration: 5

If the parameter values are perturbed slightly, a sense of the movement of the nodes is obtained by inspecting the eigenvalues. We notice that for E_3, $\lambda_1 < 1$ and $\lambda_2 > 1$. λ_2 approaches one from above. For E_4, $\lambda_1 < 1$ and $\lambda_2 < 1$. λ_2 approaches one from below, while λ_1 stays significantly less than 1. As E_3 approaches a state of stability, $\lambda_1\lambda_2 < 1$, and E_4 approaches a state of instability, $\lambda_2 = 1$, the two nodes collide giving way to the last case of equilibria $B^2 = 4AC$ which we will call $E_\star$. This is the dividing point, bifurcation between two positive real roots, and two imaginary roots.

This is a special case when $E_\star$ becomes a saddle node bifurcation. In order to study the

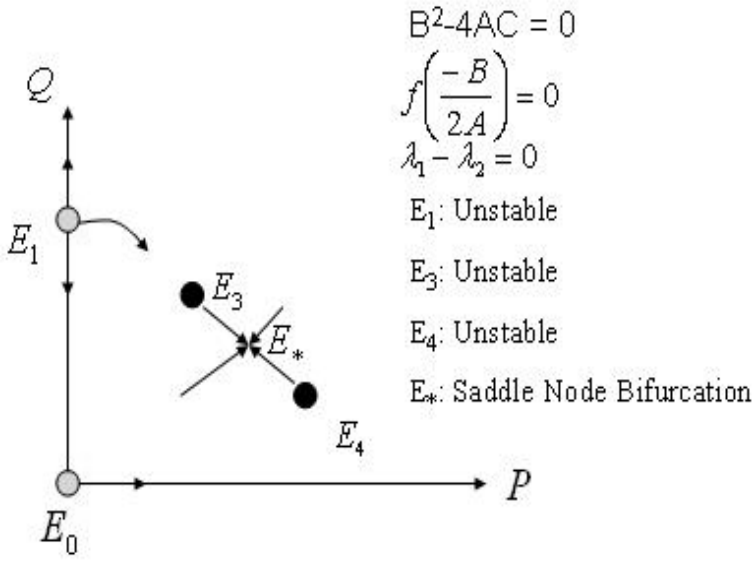

Illustration: 6

sensitivity of the occurrence of the saddle node bifurcation, sensitivity analysis is performed to determine which parameter(s) have the greatest impact in the change of stability of the existing equilibrium points.

6 Sensitivity Analysis

The sensitivity of the existence of the saddle-node bifurcation is explored by studying the possible scenarios for which the parabola described in Illustration 7 gives either two steady states (one stable and one unstable) or a single steady state in which the previous steady state coalesce to create a saddle-node bifurcation. In particular, the sensitivity to the occurrence of the saddle-node bifurcation can be used to describe the function h (where h is the maximum value attained by the parabola).

Let

$$h = F\left(\frac{-B}{2A}\right) = \frac{4AC - B^2}{4A}$$

be the quadratic function in Illustration 7 evaluated at the vertex $\frac{-B}{2A}$. To explore the sensitivity of h to the variability of the parameters in the proposed models, let ξ represent any of the seven parameters (a, b, m, c_{ij} for $i, j = 1, 2$). Consider a small perturbation to ξ by $\Delta\xi$. A perturbation in ξ suggests that a perturbation will affect h (ξh) as well. The normalized sensitivity index $\mathcal{S}_\xi$ is the ratio of the corresponding normalized changes. The sensitivity index for parameter ξ is defined as

$$\mathcal{S}_\xi := \frac{\Delta h}{h} / \frac{\Delta \xi}{\xi} = \frac{\xi}{h}\frac{\partial h}{\partial \xi}$$

The indices $\mathcal{S}_\xi$ were calculated for the parameters in our model. Considering h and calculating the sensitivity for each of its seven parameters, the following normalized sensitivity indices are obtained:

Sensitivity of Parameters

F	S_a	S_b	S_m	$S_{c_{11}}$	$S_{c_{12}}$	$S_{c_{21}}$	$S_{c_{22}}$
$\frac{B^2-4AC}{A^2}$	-6.7692	4.9230	214.6741	0.01	0.12	0.1	0.01
$\frac{4AC-B^2}{4A}$	-6.7692	4.9230	0.6386	0.01	0.12	0.1	0.01
$\frac{-B}{2A}$	2.1458	-0.2083	-1.6806	0.01	0.12	0.1	0.01
$am - 1 - \frac{c_{11}(b-1)}{c_{22}}$	-5.6666	6.6666	2	0.01	0.12	0.1	0.01
$\frac{-B-\sqrt{B^2-4AC}}{2A}$	$1.7142 - 1.4833i$	$-4.8194 \times 10^{-12} + 0.7161i$	$-1.6806 - 22.8675i$	0.01	0.12	0.1	0.01
$\frac{-B+\sqrt{B^2-4AC}}{2A}$	$1.7142 + 1.4833i$	$-4.8194 \times 10^{-12} - 0.7161i$	$-1.6806 + 22.8675i$	0.01	0.12	0.1	0.01

[1]

Case I:

$$h = F\left(\frac{-B}{2A}\right) = \frac{4AC - B^2}{4A}.$$

When $F' < 0$, we have the vertex of the parabola approaching $F(Q) = 0$ and thus $B^2 = 4AC$.

Case II: Another way to create $B^2 = 4AC$ is to consider

$$G(Q) = |Q_2 - Q_1| = \frac{B^2 - 4AC}{A^2}$$

When $G' < 0$, we have the two roots colliding to create one root. Now we must consider that when $F' < 0$ does not guarantee $G' < 0$ simultaneously, i.e. just because the vertex is decreasing does not strictly imply that the distance between the two roots is decreasing and vice versa. However, we are only concerned with $Q_2 - Q_1 = 0$ and G. G contains seven parameters, a, b, m, c_{11}, c_{12}, c_{21}, c_{22}. If we analyze the sensitivity of G to the variability of each parameter, we find the parameters that affect G the most. Our results show that G is most sensitive to the variability of m (214.7). The sensitivity of F with respect to m is relatively small in comparison to the sensitivity of G with respect to m. Possible table results show that the value of m has the most influence in bringing about the coalescence of E_3 and E_4.

[1] $\xi = [a,b,m,c_{11},c_{12},c_{21},c_{22}]$

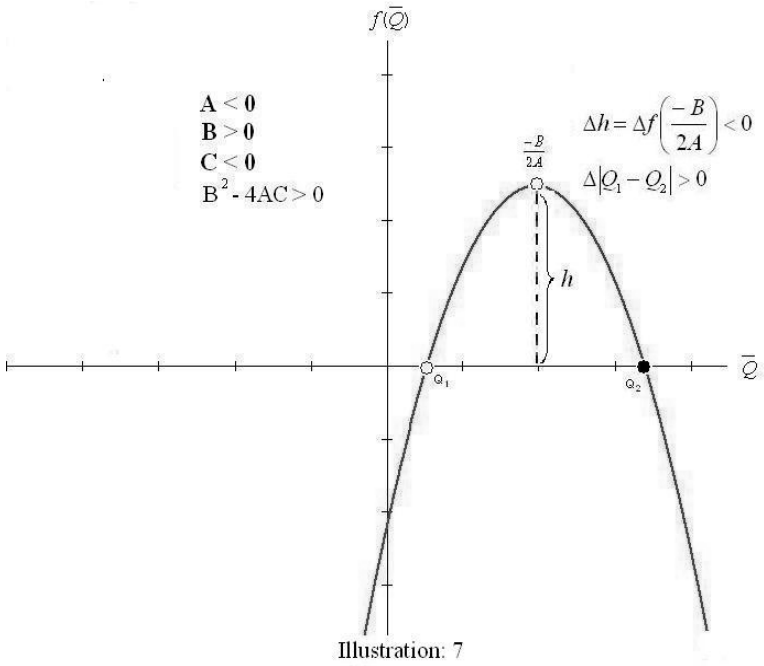

Illustration: 7

7 Stage-Structured Model

A stage structured model is introduced as an alternative to the discrete competition model. For this model, the continuous variable mean expression ratio χ_i/χ_a is partitioned into a set of four classes where χ_i and χ_a represent genes on the inactive and active χ chromosomes of the female mice respectively. This classification, while arbitrary, is important as it allows the various stages to possess different vital rates. The four stages (classes) for this model are:

1. Stage 0 Cells: Stem cells, $\frac{\chi_i}{\chi_a} = 0$
2. Stage 1 Cells: $\frac{\chi_i}{\chi_a} < 0.5\%$
3. Stage 2 Cells: $0.5\% < \frac{\chi_i}{\chi_a} < 2\%$
4. Stage 3 Cells: $\frac{\chi_i}{\chi_a} > 2\%$

Due to spatial constraints, the exact implementation of this model is given in the appendix but a few general comments will be provided. This stage structured model, once again, is a discrete time model where the number of cells in stage i at time $t+1$ depends on the number of cells in stages $i-1$ and i at time t. The projection interval, $[t, t+1]$, is taken to be one week. This structured model cannot be implemented as a simple projection matrix of the form $N_{i,t+1} = AN_{i,t}$ where A is a projection matrix (e.g. Leslie matrix) as cells can remain in a single class for many generations. In particular, cells in class i for $i = 1, 2$ have a certain probability of a transition into the next class. This transition is dependent on an increase in mean expression

ratio. This ratio increases in time during the process of mitosis. This increase is assumed to be a nonlinear process as the probability of creating further error, given a certain amount of initial error, increases with an increase in initial error due to the decrease in the amount of telomeric DNA occurring during mitotic events [7]. This creates an age distribution within the classes which may or may not be stable. Assuming that it is stable, progression of an expected number of cells into the next class is only a reasonable approximation for an initial vector near the stable age distribution. It cannot be assumed that this vector is known.

Since there are only four stages, the possibility of cells skipping classes upon transition is not considered. It is also assumed that all cells divide one time in the projection interval and that each division produces two new cells. In the case of the two cells produced by stem cells, one of the cells produced is a stem cell (exact replication with telomerase) while the other is a first generation differentiated cell in class 1 (nearly identical daughter cell). As a result of this process, the number of cells in each class (aside from the stem cells) grows exponentially in time. The number of stem cells within the organism is assumed to be a constant. Despite this unrealistic sustained exponential growth, the stage distribution or frequency of each stage within the total population is examined as it evolves in time. Lastly, cells in the last class must remain in this class or be removed from the system with increasing probability due to death (e.g. apoptosis). To run a sample of this model, functions, g_i, are chose to dictate how differentiated cells in class i will transition. The choice of g_i is arbitrary with the only constraint being that it be monotonically decreasing. After running a simulation for 100 generations (approximately two years) with an initial vector of the form $(100, 1000, 0, 0)^T$, it is observed that from generation 1 to generation 20, a 3% decrease (100-97%) in the frequency of class 1 within the population occurs. By generation 36, only 73% of the population in class 1, while 26% of the population is in class 2. At generation 59, only 27% of the population remains in class 1, while 70% is in class 2. An accumulation of cells in class 3 begins to occur with almost 2% of the population residing there. By the time the last generation of the simulation is reached, 90% and 9% of the population are in classes 2 and 3 respectively while less than 1% of the population remains in classes 0 and 1.

These results are relatively consistent with the data obtained in the experiments of Bennett-Baker *et al.* [3] in the sense that it takes many generations for cells with comparatively high amounts of error to accumulate. Since the functions g_i can be any monotonically decreasing functions, it may be possible to fit the data with more precision as these functions are altered. In particular, the strength of the nonlinear decrease is crucial in determining the evolution of stage transitions. Since this stage structured model is a work in progress it may be prudent to switch to a more manageable PDE model where age is a continuous variable. The algorithm used to create basic simulations is highly recursive and cannot be easily extrapolated to higher dimensional systems. Furthermore, this model is also biologically deficient in that there is no density or time dependence. Specifically, for future work, we would like to introduce density dependent births and time dependent births associated with stem cells. This time dependence would incorporate the idea that stem cells progressively produce first generation differentiated cells with more error (i.e. cells in higher classes). This time dependent process may create different transient dynamics than those discovered in the basic simulation used in this study.

8 Discussion

The initial purpose of this study was to develop a mathematical model that would accurately describe the work of Bennett-Baker *et. al* [3] as well as to understand the process of aging as a function of time with more accuracy. To do this, two discrete time models were constructed. The analysis of the competition model gave rise to some interesting mathematical dynamics. However this model was constructed on simple biological foundations with competition as the main interaction between cells. In particular, only two classes were used and the exact definitions of these classes is not altogether clear. Aside from this insufficiency, biological assumptions proposed may be inaccurate for the process of aging. First, we had to assume that error-free cells that produced errored cells competed in the same way as the errored cells. This assumption produced a tractable model but also indicates the need for a higher dimensional model where error-free cells that produce error-free versus errored cells are biologically distinct and thus belong in different classes governed by different interactions of varying strengths. Second, it is also important to incorporate demographic stochasticity in the model as there are variations within individuals in the two classes. Depending on the magnitude and placement of stochastic events within the model, the long term dynamics may be variable and resemble the distributions seen in the data. Despite these shortcomings, the model was instructive through the mathematical analysis. We feel confident that we have completely described all of the nonlinear phenomena predicted by this model for various parameter values. Although we have no proof of this, both analytical and numerical results strongly suggest this. If such a complete characterization is true, this model may be of future use to mathematical modelers.

The stage structured model we constructed was more biologically accurate than the competition model because of the addition of more classes. This allowed for the differentiation of the vital rates of cells in different stages. This, in turn, made the system much more complicated and analysis was possible only through numerical simulations. These simulations did provide a view of the frequency of cells within the stages throughout time (as conducted in the experiment). These results match the findings of the experiments of Bennett-Baker *et al.* [3] qualitatively; the expression of inactivated genes stays extremely low for an extended period of time, and then begins to increase at an increasing rate. This is due to the fact that we used a nonlinear function to dictate how cells transition from class to class. The choice of the function was arbitrary, so it is possible to fit the data more accurately with a more appropriate choices. Due to the fact that there is so little data, interpolation may vary widely. Demographic effects should also be added as variations in individuals arise in the data.

During the process of analyzing these two models, ideas for future studies of this topic arose naturally. First, evidence suggests that the equilibria of the two-dimensional model may be globally stable. Proving this may be possible using monotone map theory and would further enhance the existing results. Stage structure seems to be important to understand the aging process. Therefore, developing a PDE model may be the next natural step. Introducing time, density and demographic effects individually and in combination will also contribute to a more realistic future model.

References

[1] M. Ali, *The Oxidative-Dysoxygenative Model of Aging*, The journal of integrative medicine 7, 21-30, 2003.

[2] B. Best, *Proteins and the glycation theory of aging: Mechanisms of aging*, No date provided by author.

[3] P. Bennett-Baker, Jodi Wilkowski, David T. Burke, *Age-associated activation of epigenetically repressed genes in the mouse*, 2003.

[4] F. Brauer and C. Castillo-Chavez, *Mathematical Models in Population Biology and Epidemiology*, Springer-Verlag, 2000.

[5] J. M. Cushing, Sheree Levarge, Nakul Chitnis, Shandelle M. Henson, *Some Discrete Competition Models and the Competitive Exclusion Principle*, J. Diff. Eqns. and Appl. (in press)

[6] M. Florez-Duquet, R. B. McDonald, *Cold-induced thermoregulation and biological aging*, Physiological Reviews, Vol. 78, No. 2, 339-358, 1998.

[7] M. Fossel, M.D., Ph.D., *Can we cure aging?*, No date provided by author.

[8] L. A. Gavrilov, N.S. Gavrilova, *Evolutionary theories of aging and longevity*, The Scientific World Journal (2002) 2, 339-356, 2002.

[9] R. Gerome, Y. Hiromoto, N. Tan Abe, M. Ishida, M. Matsumoto, S. E. Lindstrom, T. Takahashi, K. Gerome, *Evolutionary characteristics of influenza B virus since its first isolation in 1940: dynamic circulation of deletion and insertion mechanism*, Arch. Vier. 143, 1569-1583, 1998.

[10] M. Kyriazis, M.D. *Cross-link Breakers and Inhibitors*, No date provided by author.

[11] S. Lehrman, *Genetics of Aging and Longetivity*, 2002.

[12] D. H. Ly, *Mitotic Misregulation and Human Aging*, Science, 287, 2486-2492, March 31, 2000.

[13] N. C. Nelson. *The free radical theory of aging*, No date provided by author.

[14] W. Dean M.D., *New Life for an Old Theory: Part 1 Crosslinkage Theory of Aging*, No date provided by author.

9 Appendix

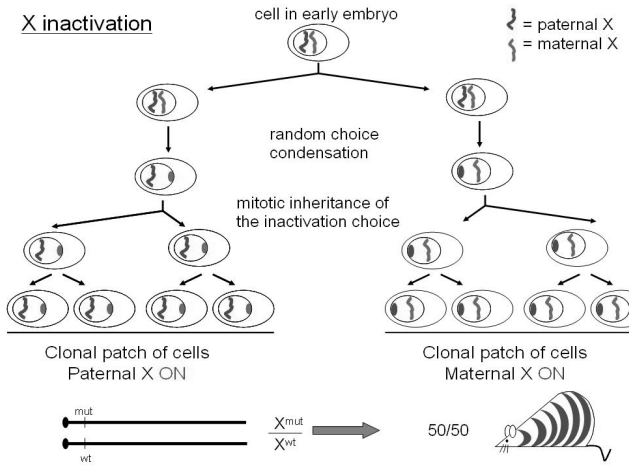

Figure 2: Inactivation of maternal and paternal X-Chromosomes.

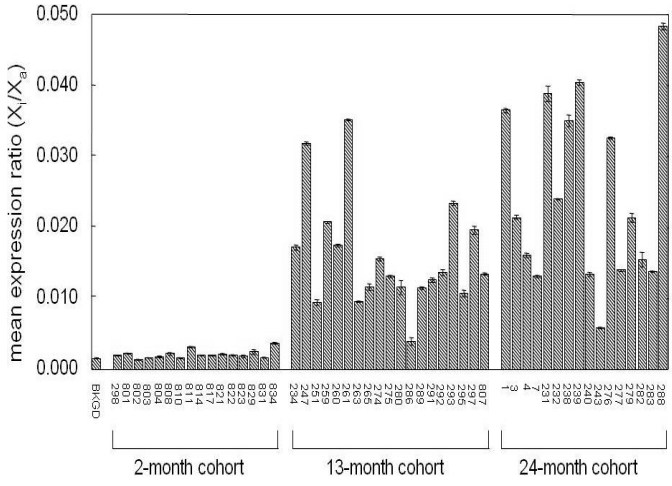

Figure 3: Atp7a gene expression in mouse spleen RNA.

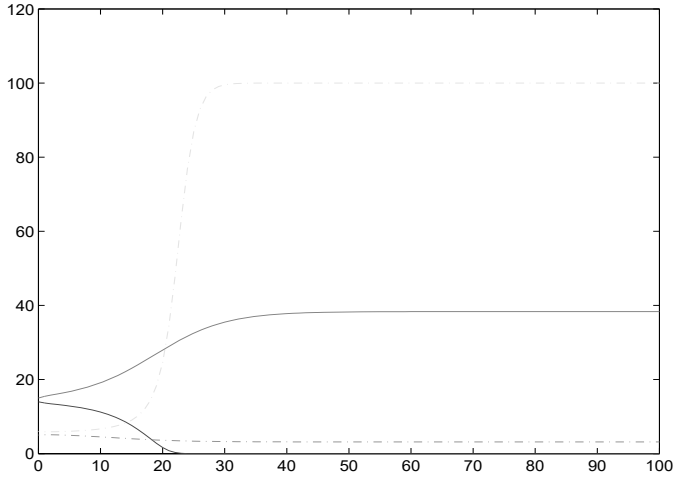

Figure 4: Bistability. Red (P) and pink (Q) time series shows the asymptotic state (coexistence) for the initial condition (15,5). Blue (P) and cyan (Q) time series shows the asymptotic state (exclusion) for the initial condition (14,6). These time series collectively show the effect of the nearby saddle node acting as a separatrix for the basins of attraction of the multiple equilibria. Parameter values used were $m = .85,\ c_{11} = .01,\ c_{12} = .1,\ c_{21} = .12,\ c_{22} = .01$.

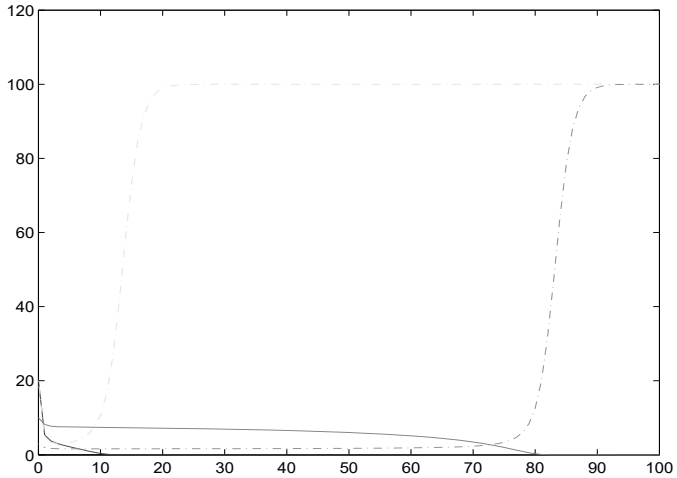

Figure 5: Time series showing the effect of the saddle node bifurcation just following criticality. The red (P) and pink (Q) transient dynamics are influenced by the remaining "ghost" of the saddle node bifurcation for the initial condition (10,3). The transient dynamics for blue (P) and cyan (Q) are not affected by this ghost for initial condition (20,20). Parameter values used were $m = .7,\ c_{11} = .01,\ c_{12} = .20185,\ c_{21} = .5,\ c_{22} = .01$.

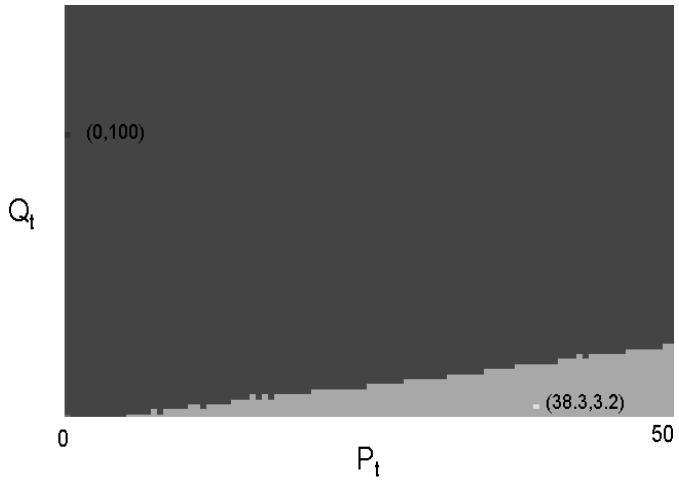

Figure 6: Attractors.

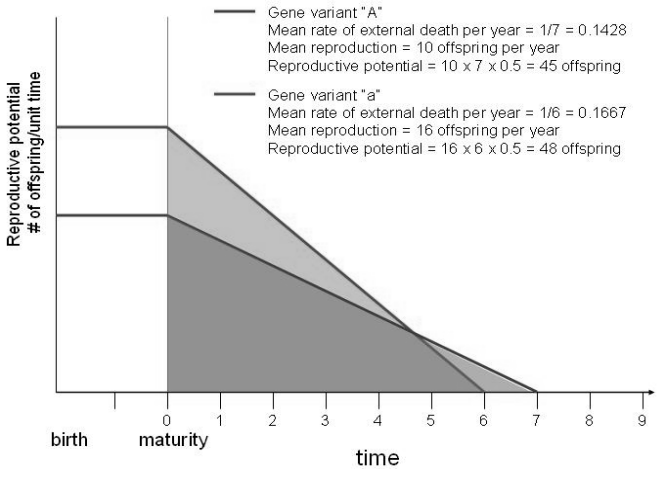

Figure 7: Impact of natural selection on reproductive potential.